Supporting Information

Carbon fabric based self-powered magnetoelectric tactile sensors for soft robot's sensing with resistances to acidic/alkaline environments

Jianyu Huang[a], Qi Wang[b], Zhenhua Wu[a], Jingyuan Zhang[c], Zheng Ma[a], Yamei Yue[a], Bin Su*[a]

[a]State Key Laboratory of Material Processing and Die & Mould Technology, School of Materials Science and Engineering, Huazhong University of Science and Technology, Wuhan 430074, Hubei, P. R. China,

[b]State Key Laboratory of Advanced Electromagnetic Engineering and Technology, School of Electrical and Electronic Engineering, Huazhong University of Science and Technology, Wuhan 430074, Hubei, China,

[c]Wuhan Britain-China School, Wuhan 430015, P. R. China

* To whom correspondence should be addressed: B. Su. (subin@hust.edu.cn)

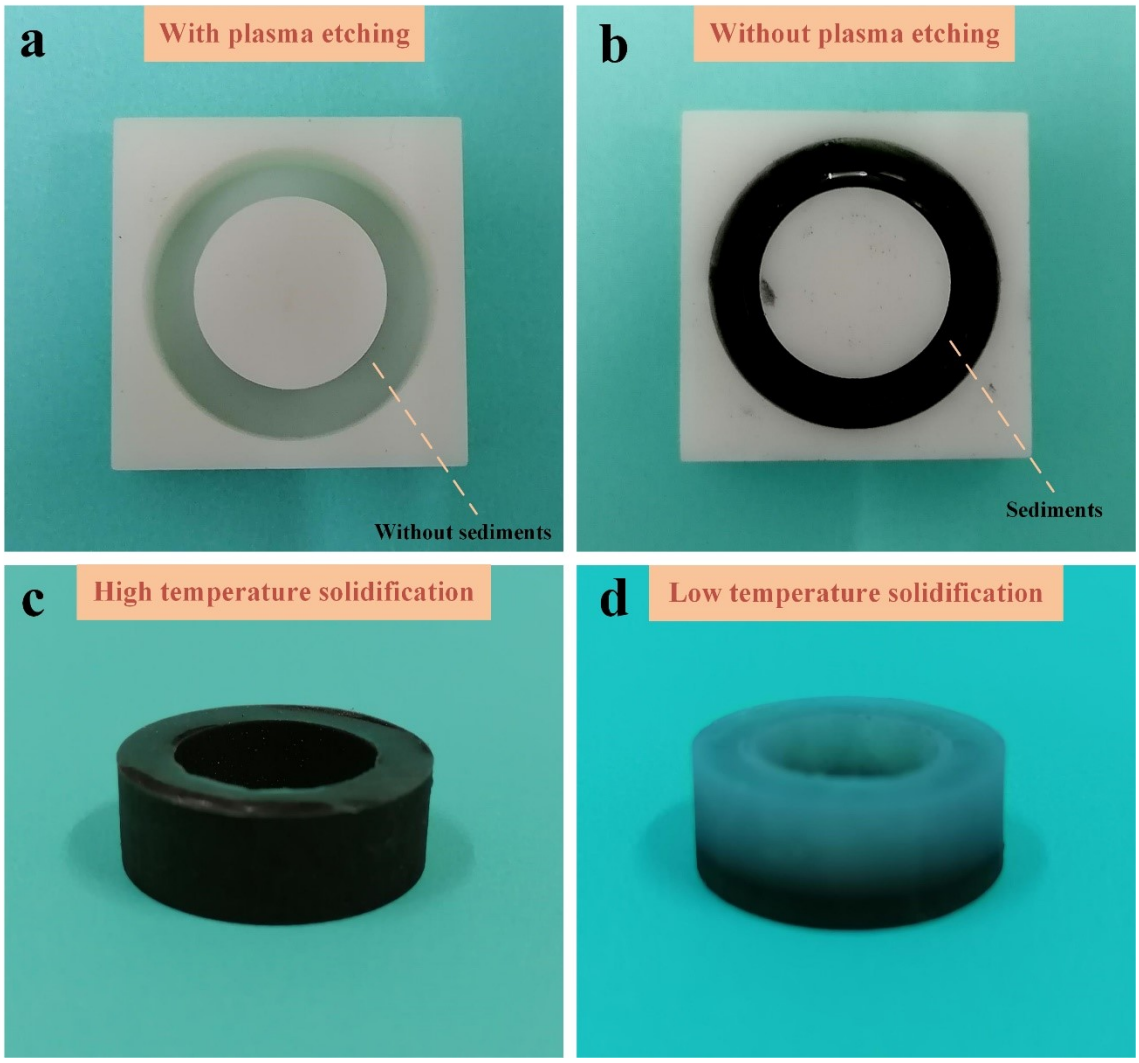

Fig. S1 Optical images of 3D-printed mold (a) with plasma etching and (b) without plasma etching after removing the magnetic elastomer. The optical images of magnetic elastomer obtained at (c) high temperature solidification and (d) low temperature solidification.

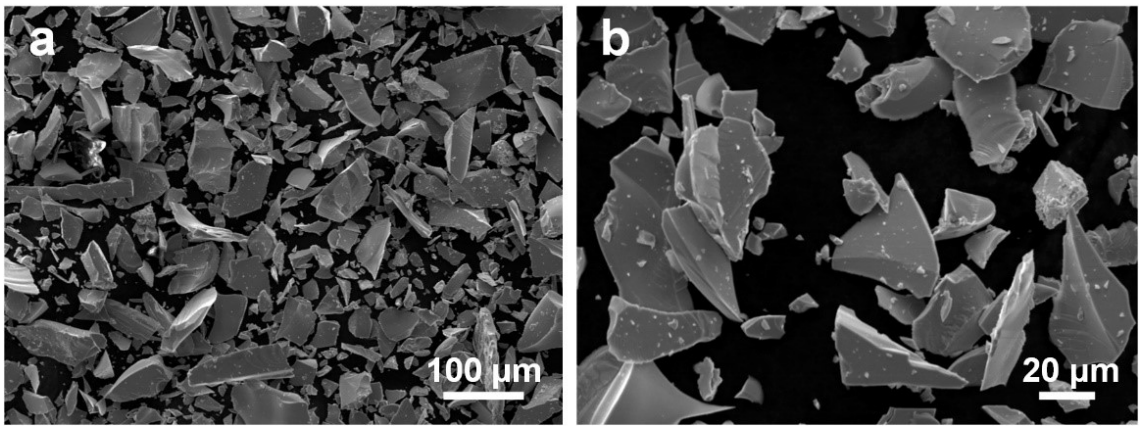

Fig. S2 (a) SEM image of magnetic microparticles and (b) corresponding magnified image of (a).

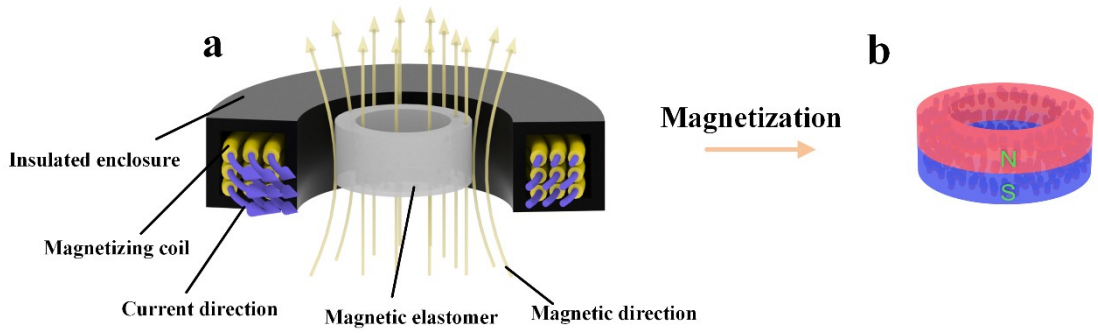

Fig. S3 (a-b) The magnetization process of magnetic elastomer.

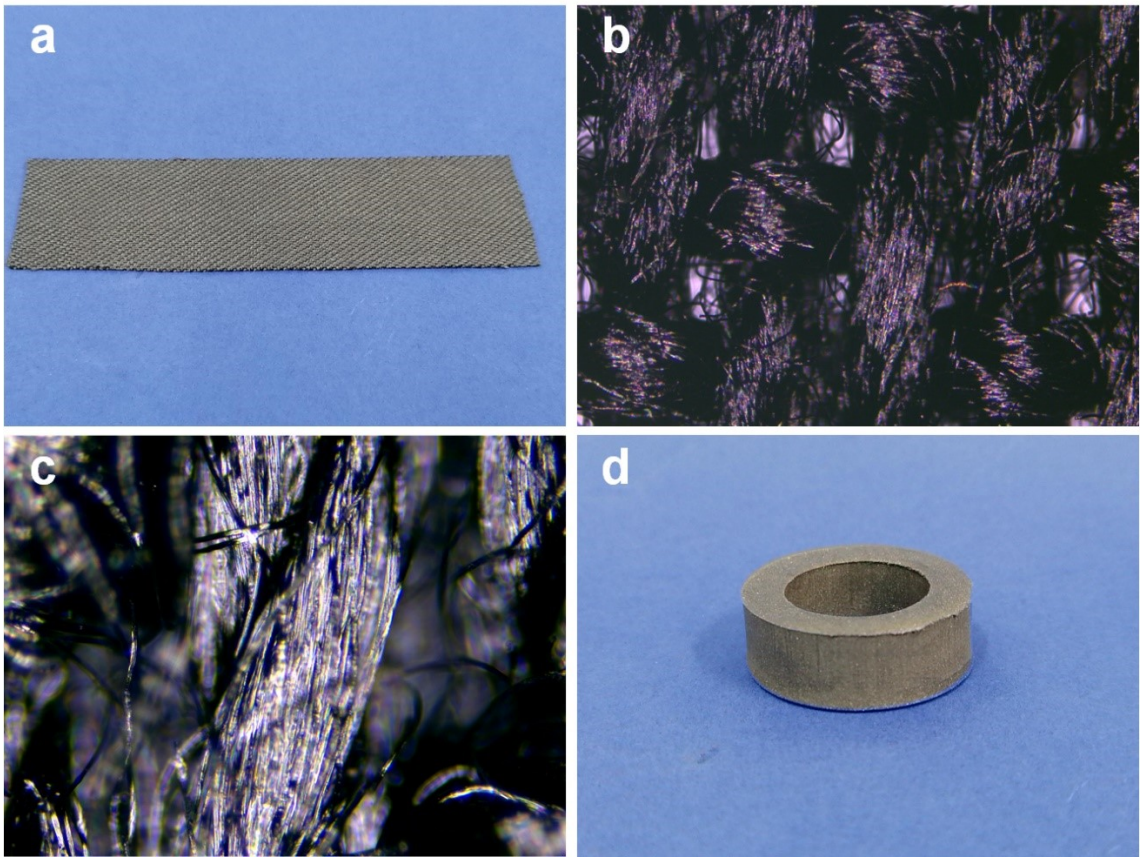

Fig. S4 Digital photograph of (a) commercial carbon cloths. (b) Optical microscope image and (c) corresponding magnified image of (b). Digital photograph of (d) magnetic elastomer.

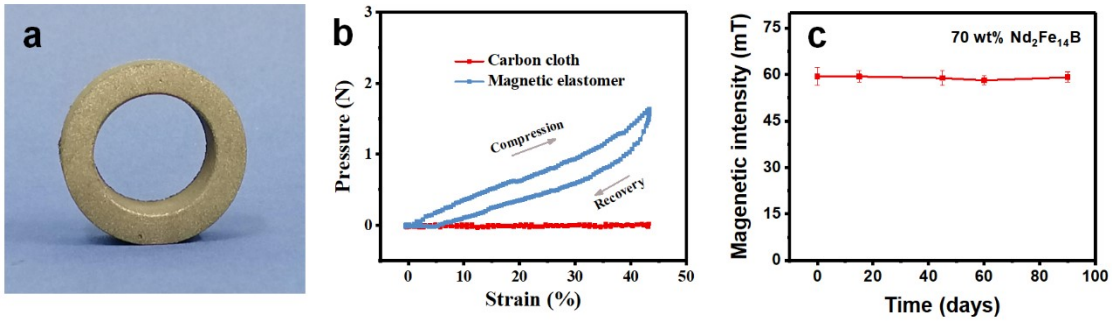

Fig. S5 (a) Digital pictures of magnetic elastomers. (b) The pressure vs strain hysteretic curve of (rea) carbon cloth and (blue) magnetic elastomers. (c) The magnetic stability of magnetic elastomer after placing on air for three months.

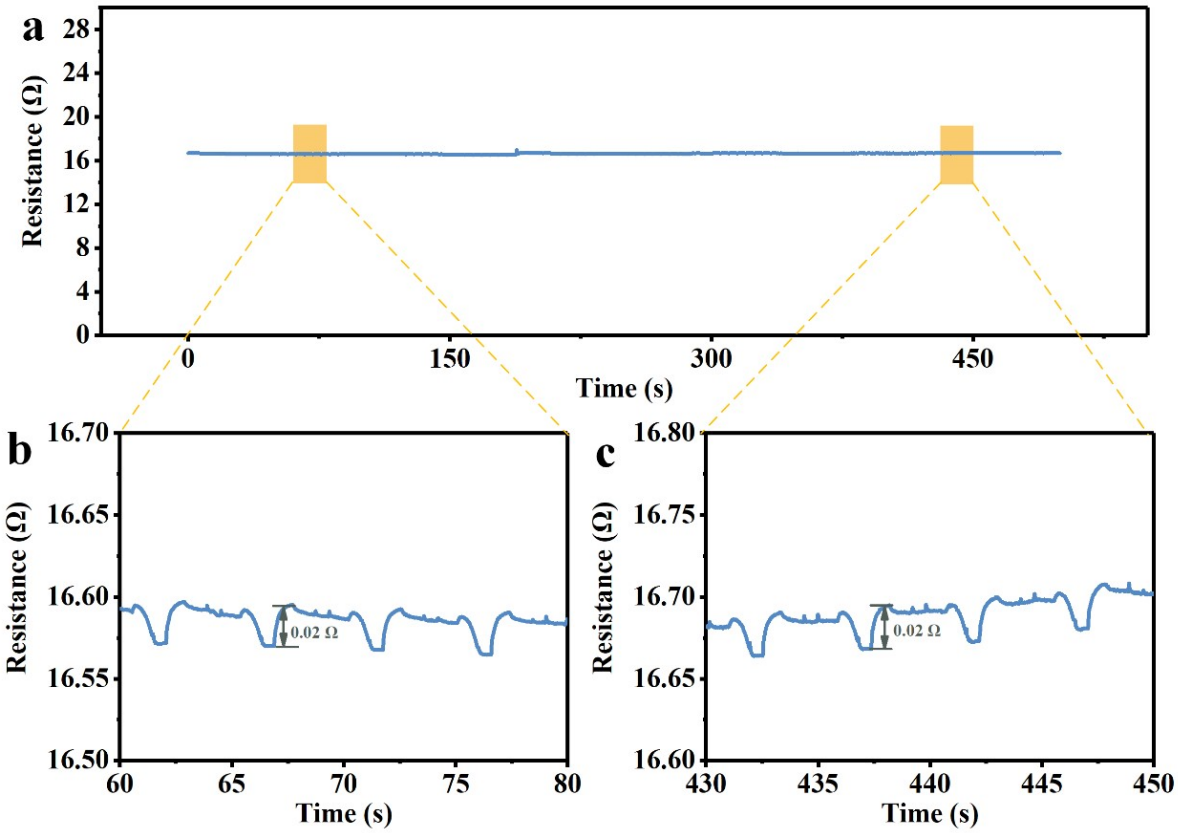

Fig. S6 (a) The resistance value change of the C-METS in the process of compression and recovery. (b) and (c) Corresponding magnified image of (a).

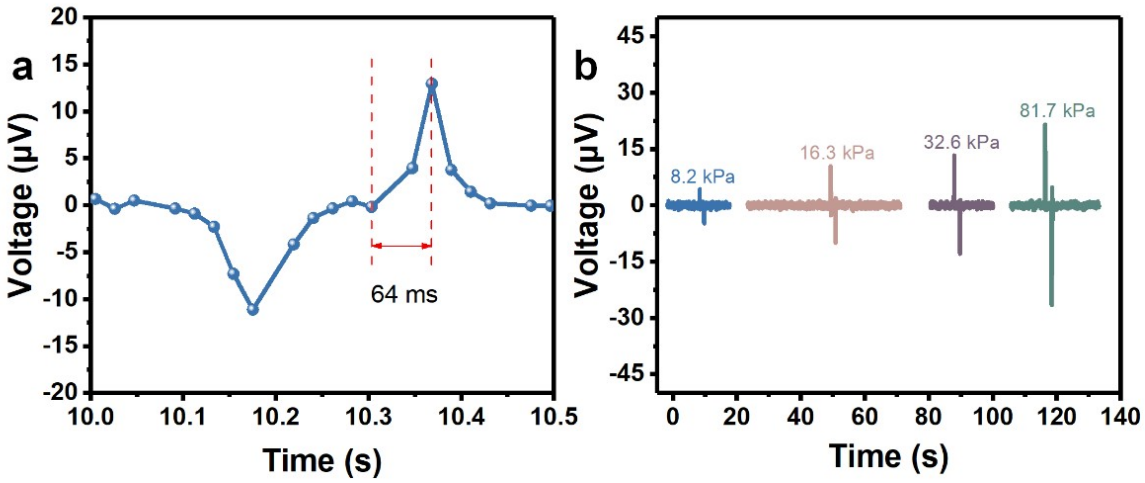

Fig. S7 (a) Instant respond of C-METS under the condition of compression frequency of ca. 2 Hz. (b) Electrical response of C-METS in different dynamic pressure.

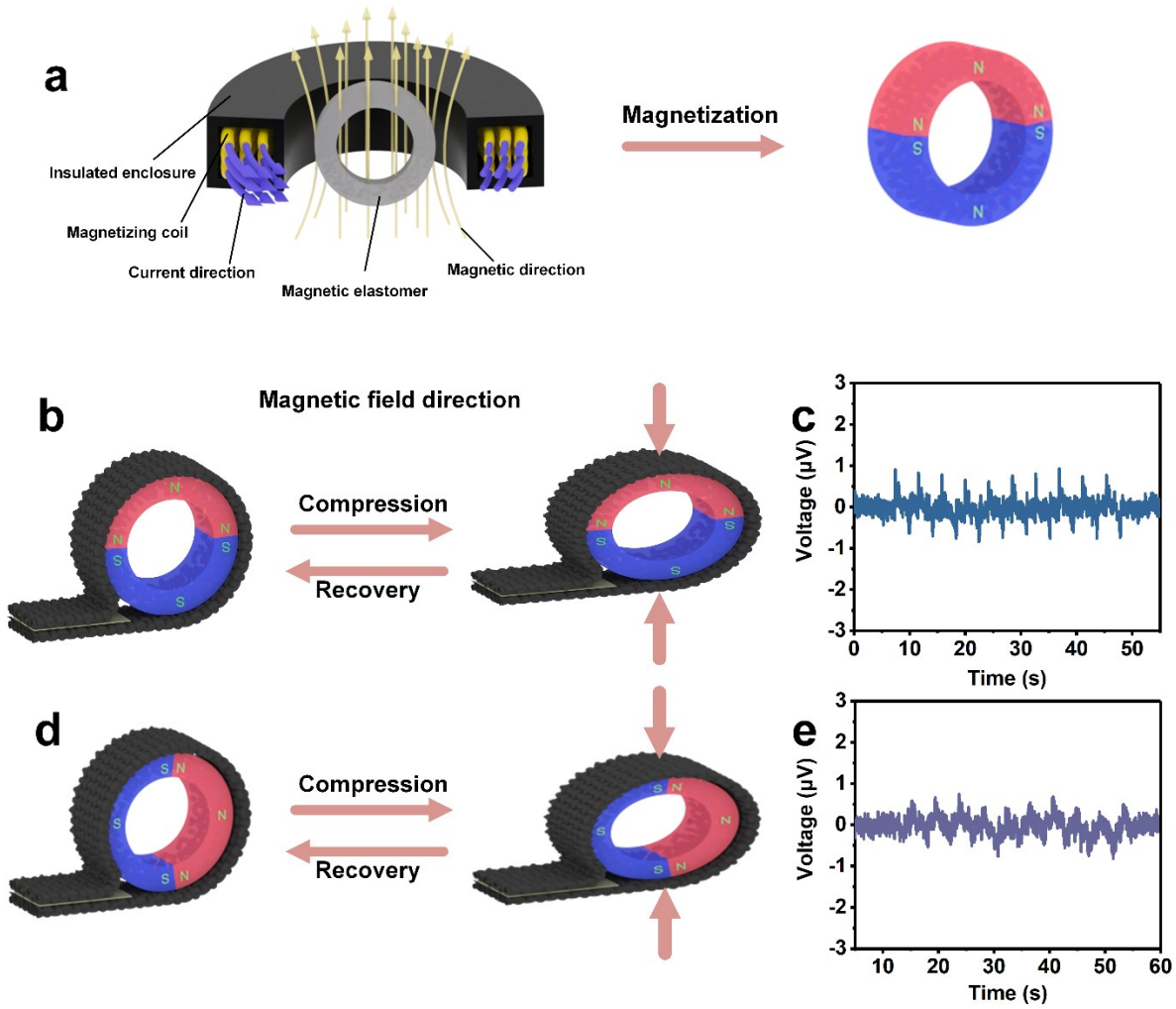

Fig. S8 (a) The magnetic elastomer is magnetized to obtain a vertical magnetic field. (b) and (d) are the schematic model for the carbon wrapping the magnetic elastomer with different magnetic field directions, respectively. (c) and (e) is the corresponding output voltage of (b) and (d) under the same test condition, respectively.

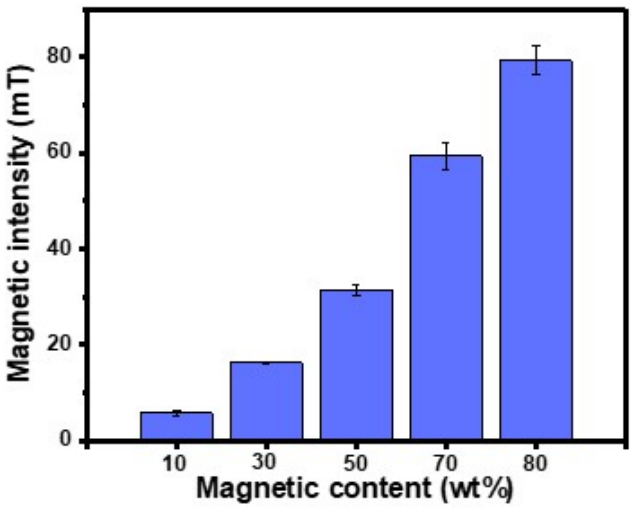

Fig. S9 The relation of different magnetic content of magnetic elastomers on their magnetic strength.

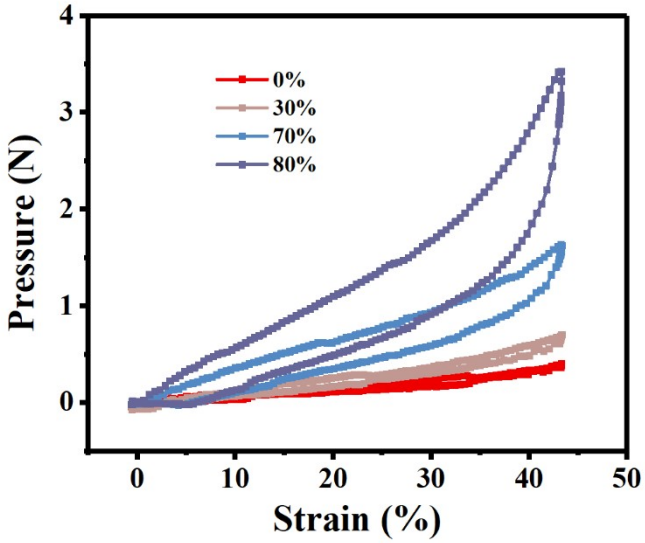

Fig. S10 The pressure vs strain curves of magnetic elastomer with different magnetic content.

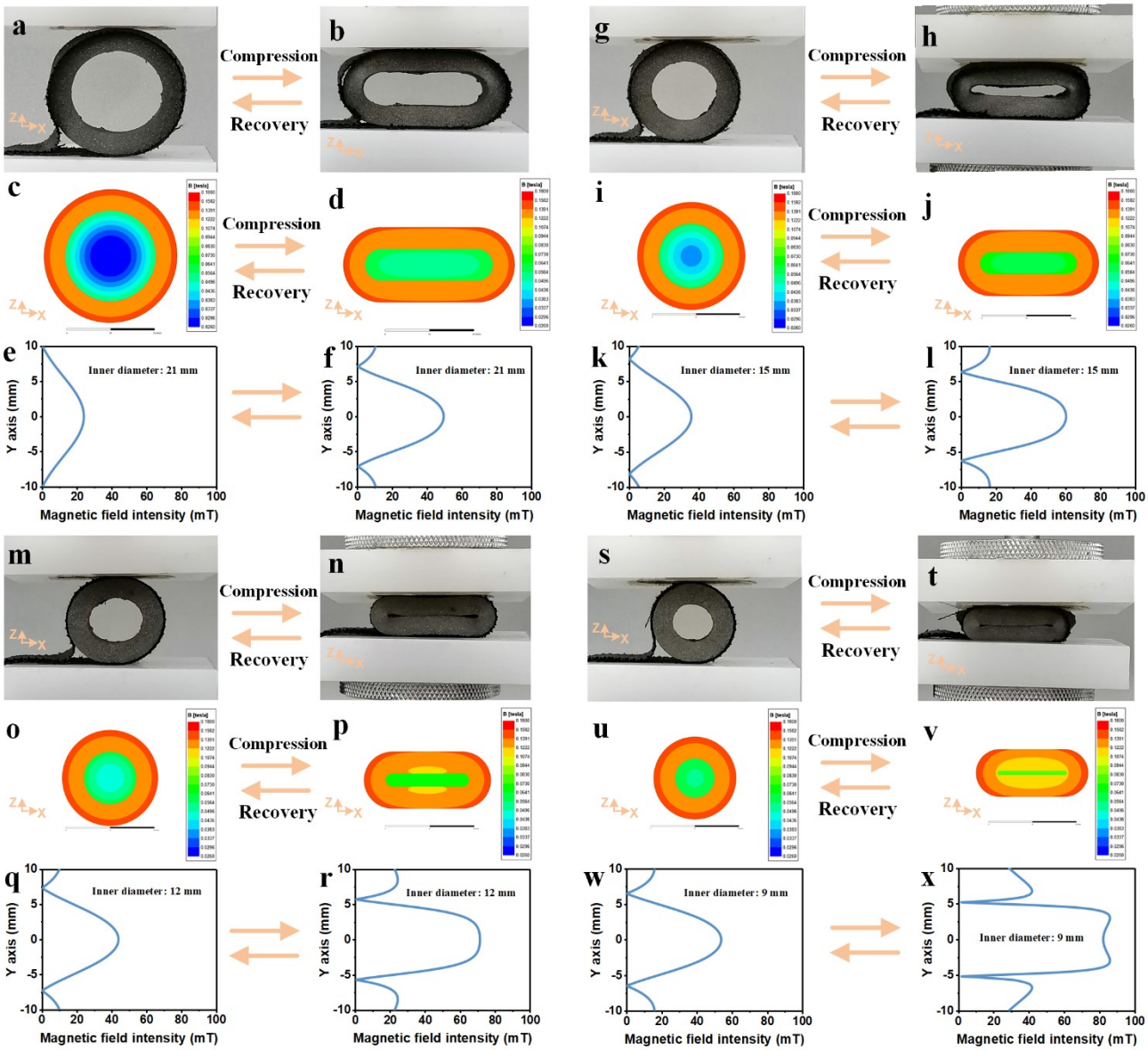

Fig. S11 (a-b, g-h, m-n and s-t) The optical image, (c-d, i-j, o-p and u-v) two-dimensional magnetic field distribution and (e-f, k-l, q-r and w-x) corresponding magnetic field intensity of different inner diameter of magnetic elastomer, when the compression distance is 12 mm and the compression speed is 800 mm min^{-1}.

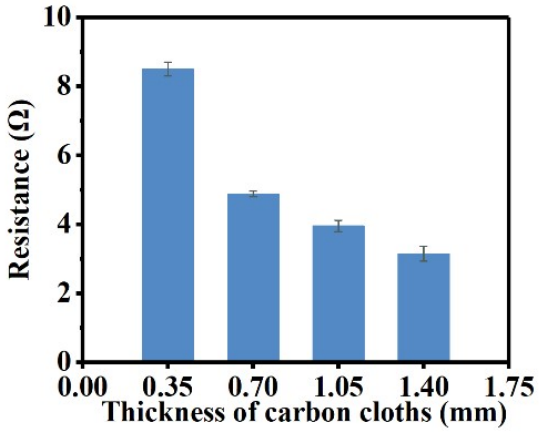

Fig. S12 Resistance value of carbon cloths with different thickness.

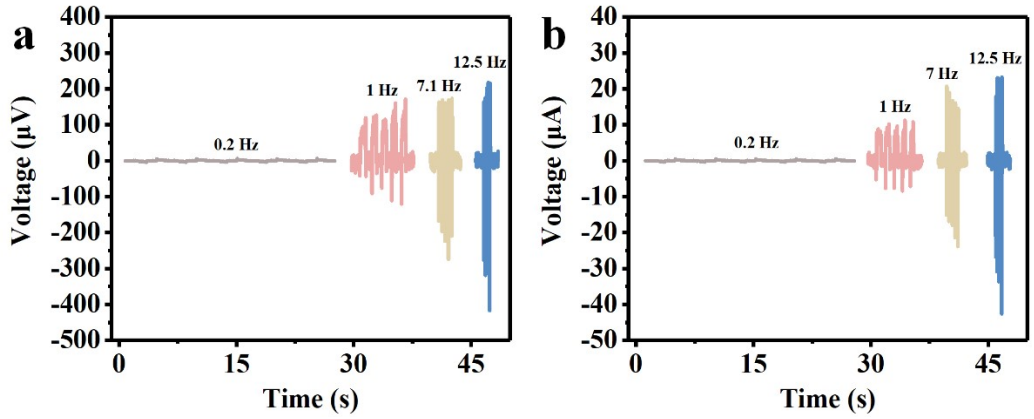

Fig. S13 The (a) voltage ang (b) current signal of C-METS at different compression frequency.

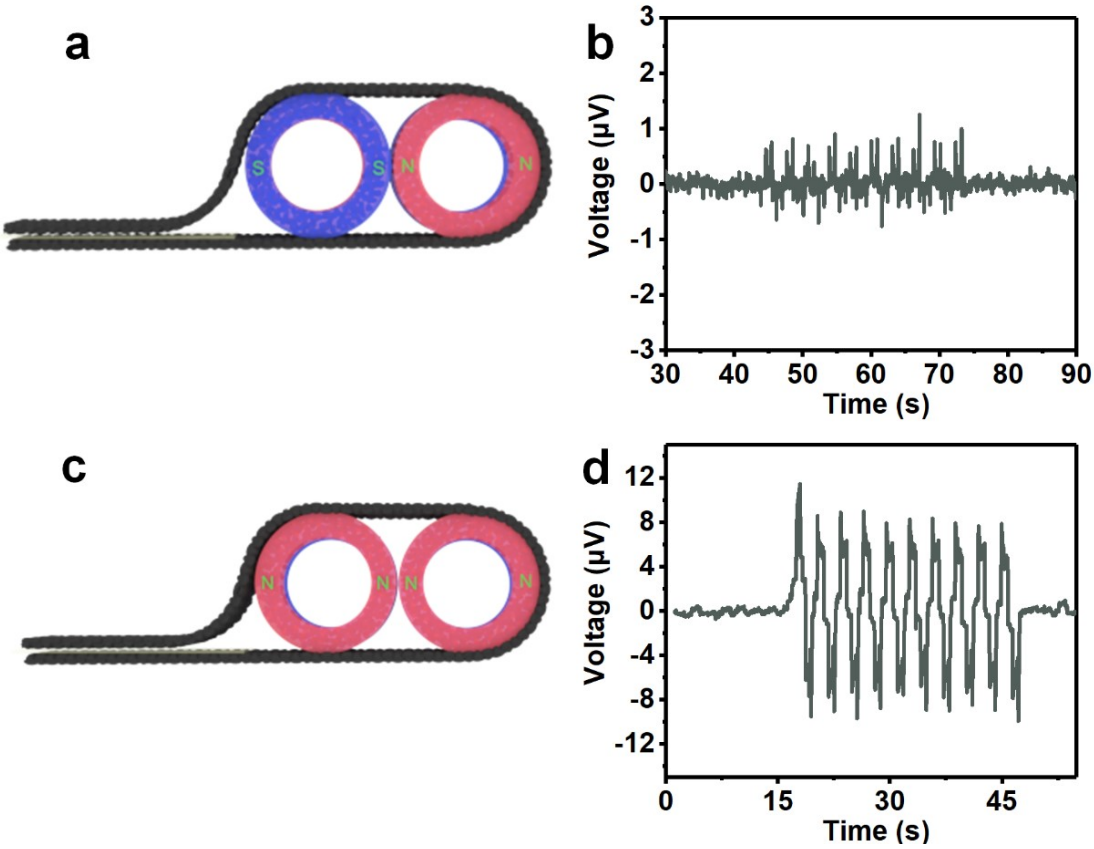

Fig. S14 (a) C-METS sensor was assembled by using two magnetic elastomers together with the opposite magnetic direction. (b) The corresponding output voltage of (a) at a compression distance of 12 mm. (c) C-METS sensor was assembled by using two magnetic elastomers together with the same magnetic direction. (d) The corresponding output voltage of (c) at a compression distance of 12 mm.

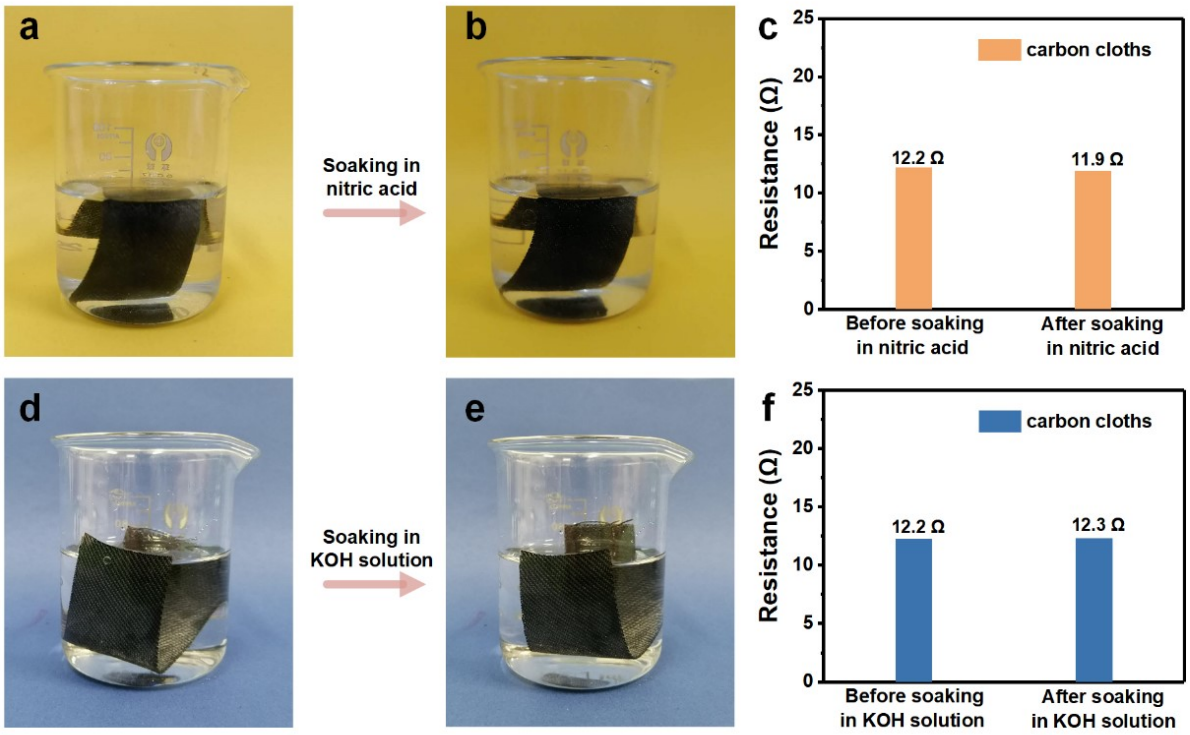

Fig. S15 Digital images of carbon cloths (a) before and (b) after soaking in 2 mol L^{-1} nitric acid solution for 6 hours. (c) The resistance value of carbon cloths corresponding to (a) and (b). Digital images of carbon cloths (d) before and (e) after soaking in 2 mol L^{-1} KOH solution for 24 hours. (f) The resistance value of copper sheets corresponding to (d) and (e).

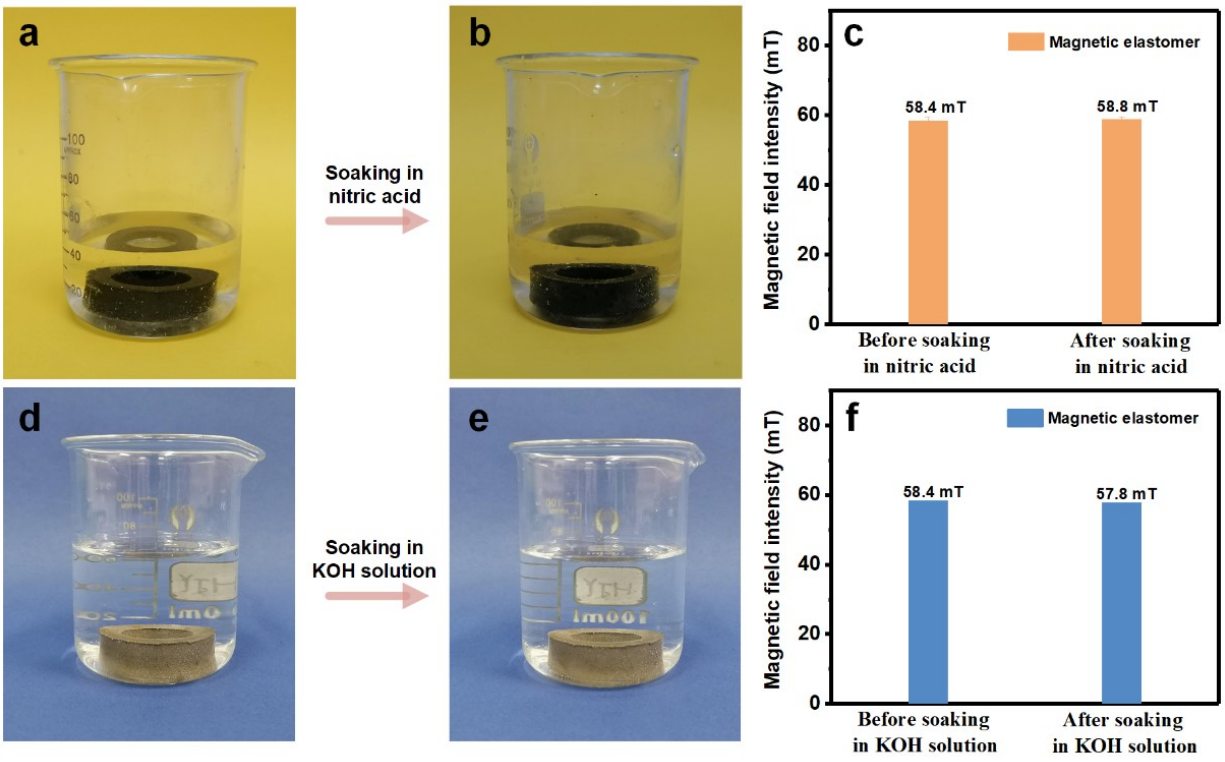

Fig. S16 Digital images of magnetic elastomer (a) before and (b) after soaking in 2 mol L^{-1} nitric acid for 6 hours. (c) The corresponding magnetic strength of (a) and (b). Digital images of magnetic elastomer (d) before and (e) after soaking in 2 mol L^{-1} KOH solution for 24 hours. (f) The corresponding magnetic strength of (d) and (e).

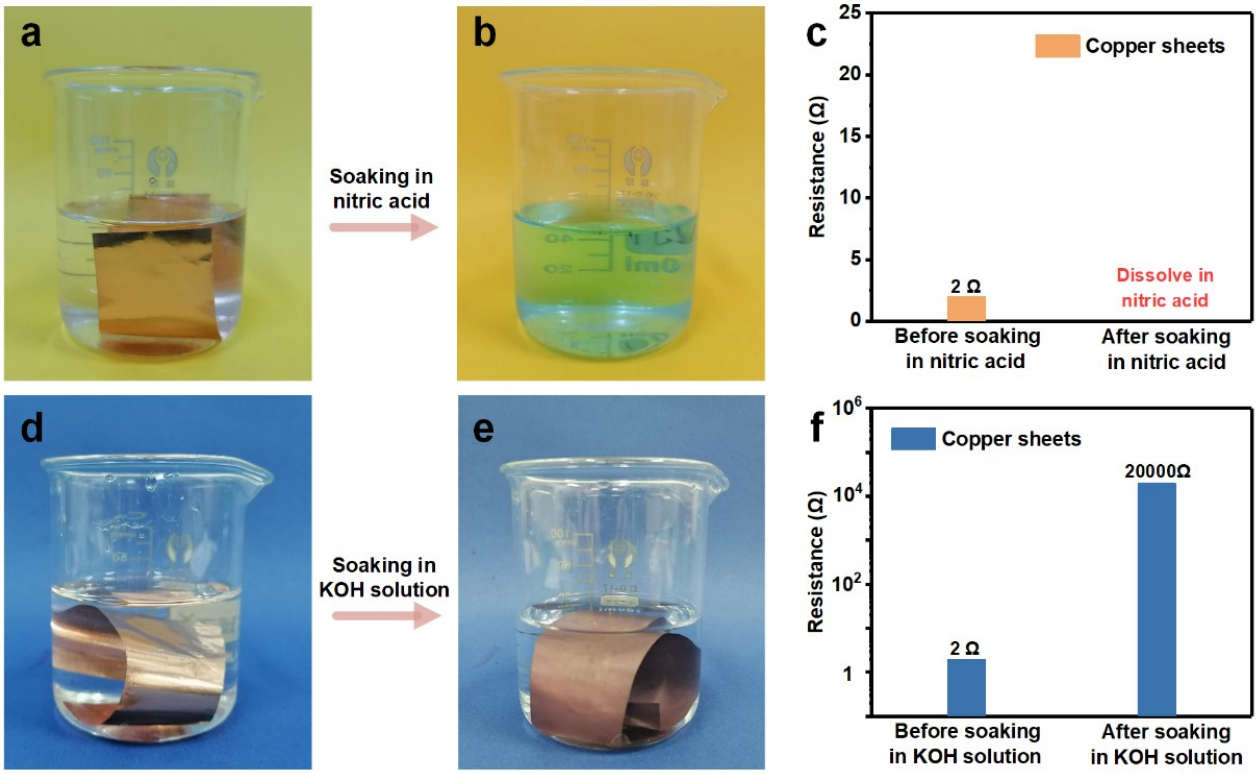

Fig. S17 Digital images of copper sheets (a) before and (b) after soaking in 2 mol L^{-1} nitric acid solution for 6 hours. (c) The resistance value of copper sheets corresponding to (a) and (b). Digital images of copper sheets (d) before and (e) after soaking in 2 mol L^{-1} KOH solution for 24 hours. (f) The resistance value of copper sheets corresponding to (d) and (e).

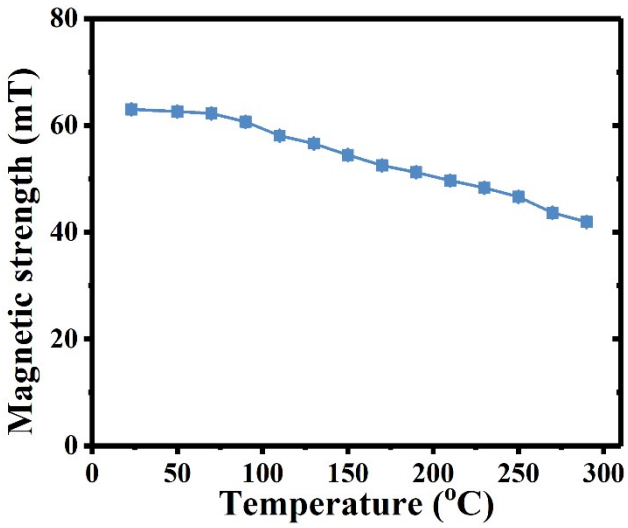

Fig. S18 (a) Magnetic strength dependence of magnetic elastomer with different environment temperature.

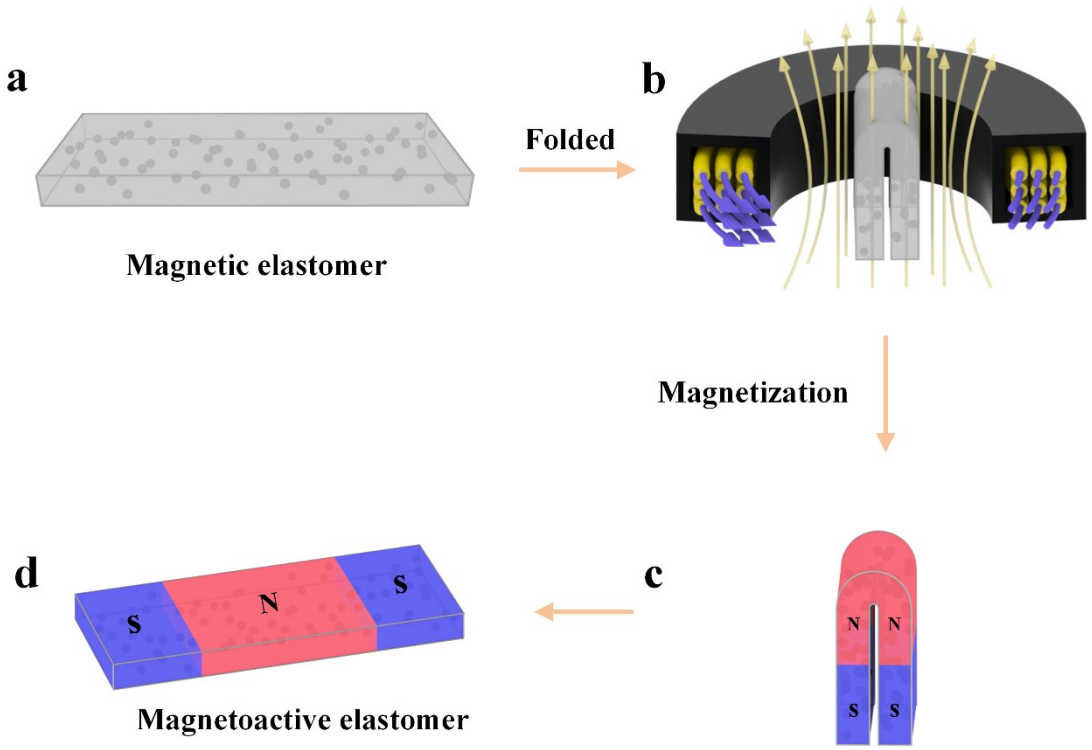

Fig. S19 The magnetization process of magnetoactive elastomer.

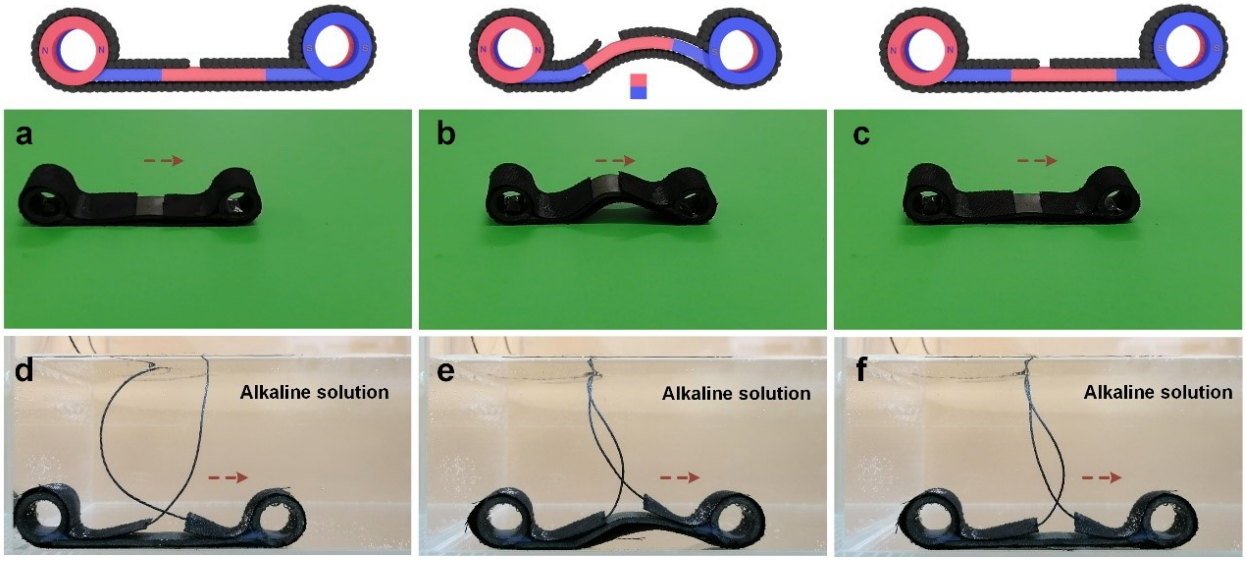

Fig. S20 Soft robot moves on the ground (a-c) and in the alkaline solution (d-f).

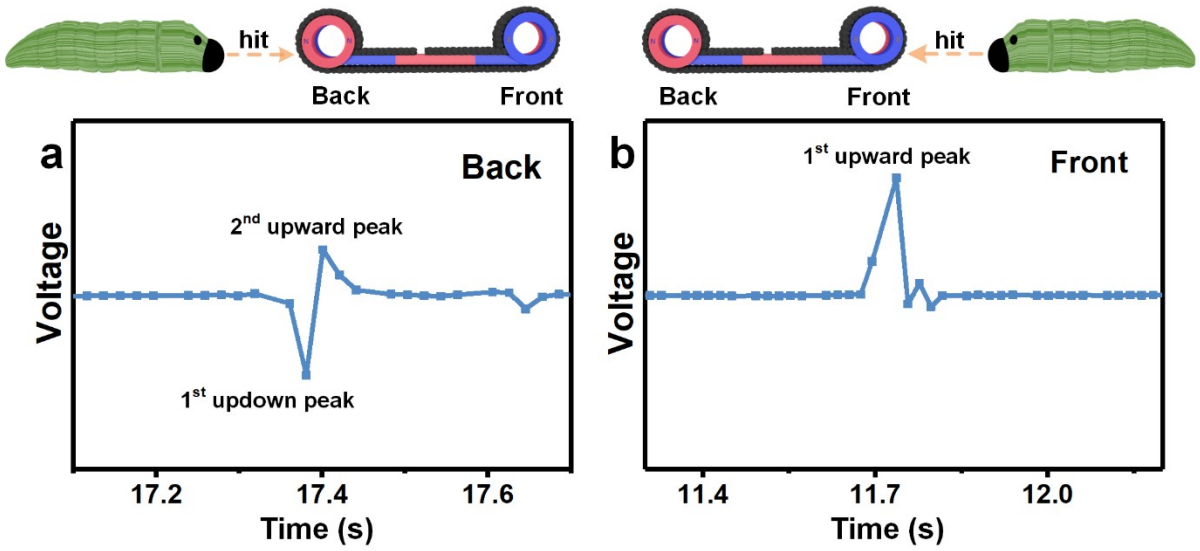

Fig. S21 The voltage signals when a worm crawled forward and hit the (a) back and (b) front of soft robot, respectively.

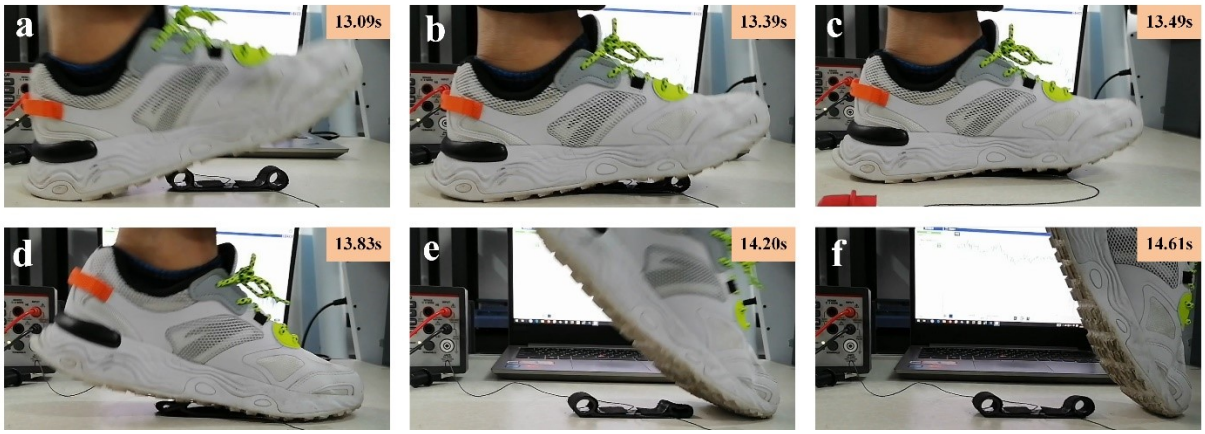

Fig. S22 The optical pictures of soft robot when a person stepping from the left side to the right side of the robot.

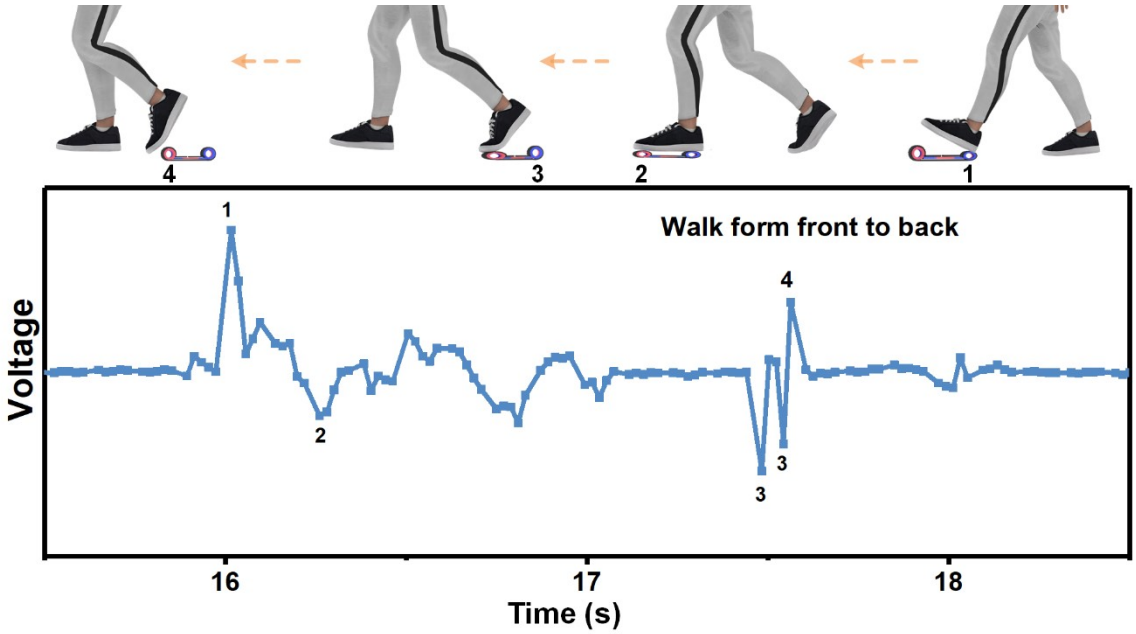

Fig. S23 The voltage signals when a person stepped from the front to the back of the robot, which could be attributed to four parts: stepping on the front (1), stepping on the back (2), leaving the front (3) and leaving the back of the soft robot (4), respectively.

Table S1. The change of total magnetic flux for C-METS with inner diameter of 18 mm before/after compression at compression distance of 12 mm.

Total magnetic flux in initial state ($\times 10^{-6}$ Wb)	Total magnetic flux in compressed state ($\times 10^{-6}$ Wb)	The change of total magnetic flux ($\times 10^{-6}$ Wb)	Output voltage calculated by simulation	Output voltage obtained by experiment
38.9	40.7	1.8	2.0 μV	2.2 μV

Table S2. The change of total magnetic flux for C-METS with different inner diameter at compression distance of 12 mm and the compression speed of 800 mm min^{-1}.

Inner diameter	Total magnetic flux in initial state ($\times 10^{-6}$ Wb)	Total magnetic flux in compressed state ($\times 10^{-6}$ Wb)	The change of total magnetic flux ($\times 10^{-6}$ Wb)	Output voltage calculated by simulation
9 mm	26.5	30.1	3.5	3.6 μV
12 mm	30.8	33.6	2.8	3.2 μV
15 mm	38.9	37.1	2.2	2.6 μV
18 mm	38.9	40.7	1.8	2.0 μV
21 mm	42.8	44.4	1.6	1.7 μV